

## CHEMICAL TREATMENT OF $\gamma$ - $\text{Al}_2\text{O}_3$ AND ITS INFLUENCE ON THE ACTIVITY, SELECTIVITY AND STABILITY OF COBALT-BASED CATALYSTS FOR FISCHER-TROPSCH SYNTHESIS

Ali Karimi

*Gas Research Division, Research Institute of Petroleum Industry, Tehran, Iran*

Received March 2, 2016; Accepted May 26, 2016

### Abstract

In this research,  $\gamma$ -Alumina was pretreated in the presence of phosphoric acid-ethanol, and then used to prepare the supported cobalt catalysts for Fischer-Tropsch synthesis (FTS). Different concentrations of phosphoric acid were applied for pretreatment of  $\gamma$ -Alumina to modify its surface properties. The catalysts were prepared by incipient wetness impregnation of the cobalt precursor. The reduction degree and dispersion of  $\gamma$ -alumina-supported cobalt catalyst were improved through this pretreatment. The obtained catalysts were characterized by FTIR, XRD, TPR, TEM and  $\text{H}_2$  chemisorption. These characterizations clearly showed the changes of morphology (surface area, pore volume, pore size distribution and crystallite phase) of the supports. The proposed modified  $\gamma$ -alumina supported catalysts increased the FTS rate from 0.062 to 0.1195 g HC/gcat./h,  $\text{C}_5^+$  selectivity increased 10% and  $\text{CH}_4$  selectivity decreased 73%, compared to that prepared by conventional  $\gamma$ -alumina support. Optimize the support pretreatment parameters exhibited significant catalyst's stability applying to FTS reaction in CSTR reactor during 320 h test.

**Keywords:**  $\gamma$ -Alumina; Cobalt catalyst; Fischer-Tropsch synthesis; Phosphoric acid; Activity and selectivity.

## 1. Introduction

There is a renewed interest in Fischer-Tropsch synthesis (FTS) in both academic and industry, largely as a result of the demand for clean and renewable transportation [1]. In the FTS reaction, syngas (a mixture of CO and  $\text{H}_2$ ), is converted into liquid fuel via catalytic surface polymerization which leads to a large variety of products such as paraffins, olefins, alcohols and aldehydes [1-3]. Supported cobalt catalysts are well-known for their activity and selectivity towards FTS. High chain growth probability, lower deactivation rates, low water-gas shift activity, and low costs make cobalt catalysts the best candidates for converting syngas to clean liquid fuels [4-5].

FTS activity of cobalt catalyst depends solely on the number of active sites located on the surface of supports, formed by reduction. The number of active sites was determined by the cobalt particle size dispersions, loading amount, and reduction degree [6-7].

Preparing impregnated catalyst is actually a complex process, in which many individual steps might influence the final performance of the catalyst, i.e., metal precursor, solvent, carrier, aging time, drying time/temperature, and calcination temperature. Failure to control these parameters might lead to irreproducible catalyst preparation. The catalytic activity and product selectivity of cobalt catalysts were affected by chemical and texture properties of the support, via their modifications on the reducibility and dispersion of cobalt or the formation of well-fined phases. Synthesis of highly dispersed cobalt catalysts requires strong interaction between the support and the cobalt precursor, but in turn, such strong interactions generally reduce reducibility of such precursors [3].

In order to achieve high surface active sites ( $\text{Co}^0$ ), cobalt precursors are dispersed on porous carriers same as  $\text{SiO}_2$ ,  $\text{Al}_2\text{O}_3$  and to a lesser extent  $\text{TiO}_2$  [5,8-9]. A drawback of these support materials is their reactivity toward cobalt, which during preparation or catalysis results in

the formation of mixed compounds that are reducible only at high reduction temperatures [5,8-9]. It is considered that the solvents, which applied to dissolve cobalt precursors or pretreat the supports, remarkably influence the interaction between the cobalt and alumina supports, meanwhile, the functional groups from solvents, formed on the surface of supports, prohibit the sintering of supported cobalt [4-6]. On the other hand, the concentration, distribution, and nature of functional groups on the alumina surface also play important role in the dispersion of supported metal on the alumina [5]. The catalytic performance of a cobalt-silica gel FTS catalyst was strongly affected by preparation condition such as pH value of solution containing precursor, because the pH value of impregnation solution changed the interaction of cobalt and silica support, resulting in different dispersion and reducibility of supported cobalt [7].

In present work, three solutions of phosphoric acid - ethanol with volume ratio of 5, 10, 15% were applied to pre-treat the alumina support, before impregnation of cobalt precursors. The different concentrations of phosphoric acid in ethanol can modify the morphology (surface area, pore volume, pore size distribution and crystallite phase) and the properties of  $\gamma$ -alumina surface, such as nature of functional group (O-P-O group), resulting in forming different catalytic property of relative catalyst. The obtained catalysts were characterized by ICP, BET, XRD, TPR, TEM, FTIR, and H<sub>2</sub> chemisorption. Finally the activity, selectivity and stability of proposed catalysts were evaluated in continuous stirred tank reactor (CSTR) and compared to catalyst prepared with the incipient wetness impregnation method on conventional  $\gamma$ -alumina. A critical discussion allows drawing useful scientific and technical conclusions.

## 2. Experimental

### 2.1. Modified alumina-support preparation

Condea Vista Catalox B-alumina (100-200 mesh, specific surface area=200 m<sup>2</sup>/g, pore volume=0.4cm<sup>3</sup>/g) was used as support materials for the preparation of cobalt FTS catalysts.

Solutions of phosphoric acid (Acros organics, 85%) in ethanol (Merck) with different concentration (vol.%) 5, 10, and 15% were prepared. 5gr extruded  $\gamma$ -alumina calcined at 500°C was immersed in solution (approximately 5 ml). This procedure followed by slow evaporating of solvent in a rotary evaporator at 60°C (approximately 3 minutes), then the support were dried in 100°C overnight in flowing air (100 ml/min), and calcined through increasing the temperature at 1°C /min from ambient to 400°C and holding for 3 h. This procedure was repeated three times and the supports named AL<sub>1</sub>, AL<sub>2</sub> and AL<sub>3</sub> for phosphoric acid - ethanol volume ratio of 5%, 10% and 15% respectively.

### 2.2. Alumina-support characterization

The surface area, pore volume, and average pore radius of the  $\gamma$ -alumina and phosphoric acid pretreated alumina (10 vol%) were measured by an ASAP-2010 system from Micromeritics. The samples were degassed at 200°C for 4 h under 50 mTorr vacuum and their BET area, pore volume, average pore radius, pore size and pore volume distributions and adsorption-desorption isotherms were determined.

### 2.3. Catalyst preparation

Cobalt catalysts (15 wt.%) were prepared by one-step incipient wetness impregnation of different modified supports (AL<sub>1</sub>-AL<sub>3</sub>) with aqueous solutions of Co(NO<sub>3</sub>)<sub>2</sub>·6H<sub>2</sub>O (Merck). The catalysts (3g) were dried in air at 100°C overnight before calcination in flowing air (100 ml/min), increasing the temperature at 1°C /min from ambient to 400°C and holding for 3 h.

The control catalyst was prepared using conventional  $\gamma$ -alumina according to procedure described above. The cobalt loading was verified by an Inductively Coupled Plasma Atomic Emission Spectroscopy (ICP-AES) system. The catalysts nomenclature and preparation's methods are reported in Table 1.

Table 1. The composition and properties of the catalysts

Catalyst / support	H <sub>3</sub> PO <sub>4</sub> used for pretreating alumina (vol.%)	P (wt.%)	Co (wt.%)	XRD $d_{Co_3O_4}$ (nm)	BET (m <sup>2</sup> /g)	Pore Volume (cm <sup>3</sup> /g)	Pore diameter (Å)
ALC <sub>1</sub>	5	0.02	14.9	16.6	165	0.323	95.9
ALC <sub>2</sub>	10	0.03	14.9	11.5	182	0.389	86.3
ALC <sub>3</sub>	15	0.05	14.8	14.4	172	0.32	100
ALCR	0	---	14.9	18.4	158	0.37	84.6
γ - Alumina	---	---	---	---	200	0.4	91.3

## 2.4. Catalyst characterization

Morphology of all catalysts (ALC<sub>1</sub>-ALC<sub>3</sub> and ALCR) were characterized by transmission electron microscopy (TEM). Sample specimens for TEM studies were prepared by ultrasonic dispersion of the catalysts in ethanol, and the suspensions were dropped onto a carbon-coated copper grid. TEM investigations were carried out using a Philips CM120 (100 kV) transmission electron microscope equipped with a NARON energy-dispersive spectrometer with a germanium detector.

The FTIR absorption technique for confirming the formation of functional groups was conducted on a Bruker ISS-88. A smooth transparent pellet of 0.5-5 % of γ-alumina mixed with 95-99.5% Potassium Bromide (KBr), was made and the infrared beam passed through this pellet.

The surface area, pore volume, and average pore radius of the γ-alumina and all catalysts were measured by an ASAP-2010 system from Micromeritics. The samples were degassed at 200°C for 4 h under 50 mTorr vacuum and their BET area, pore volume, and average pore radius were determined.

XRD measurements of the γ-alumina and calcined catalysts were conducted with a Philips PW1840 X-ray diffractometer with monochromatized Cu/Kα radiation. Using the Scherrer equation, the average size of the Co<sub>3</sub>O<sub>4</sub> crystallites in the calcined catalysts was estimated from the line broadening of a Co<sub>3</sub>O<sub>4</sub> at 2θ of 36.88°. In addition, a K factor of 0.89 was used in the Scherrer formula. The Co<sub>3</sub>O<sub>4</sub> particle size was converted to the corresponding cobalt metal particle size according to the relative molar volumes of metallic cobalt and Co<sub>3</sub>O<sub>4</sub>. The resulting conversion factor for the diameter of a given Co<sub>3</sub>O<sub>4</sub> particle  $d_{Co_3O_4}$  being reduced to metallic cobalt is [11]:

$$d_{Co^0} \text{ (nm)} = 0.75 \times d_{Co_3O_4} \quad (1)$$

Temperature programmed reduction (TPR) spectra of the catalysts were recorded using a Micromeritics TPD-TPR 2900 system, equipped with a thermal conductivity detector. The catalyst samples were first purged in a flow of argon at 400°C, to remove traces of water, and then cooled to 40°C. The TPR of 50 mg of each sample was performed using 5 % hydro-gen in argon gas mixture with a flow rate of 40cm<sup>3</sup>/min. The samples were heated from 40 to 900°C with a heating rate of 10°C/min.

The amount of chemisorbed hydrogen (H<sub>2</sub>) on the catalysts was measured using the Micromeritics TPD-TPR 2900 system. 0.25 g of the calcined catalyst was reduced under H<sub>2</sub> flow at 400°C for 20 h and then cooled to 70°C, still kept under H<sub>2</sub> flow. Then the flow was switched to Ar at the same temperature; this step, used to remove the physisorbed H<sub>2</sub>, lasted for about 30 minutes. The subsequent temperature programmed desorption (TPD) of the samples was obtained by increasing the temperature of the samples, at a ramp rate of 20°C/min, to 400°C under Ar flow. The resulting TPD spectra were used to determine the cobalt dispersion and its surface average crystallite size. The % dispersion and particle diameter are calculated by the equations have been presented in our previous work [12].

## 2.5. Catalyst activity test

The catalysts were evaluated in terms of their FTS activity (g HC produced/g cat./h) and selectivity (the percentage of the converted CO that appears as a hydrocarbon product) in a continuous stirred tank reactor (CSTR) as shown in Figure 1. The volume of CSTR was totally 1 liter. Prior to the activity tests, the catalyst activation was conducted according to the following procedure. The catalyst (10 g) with 4 - 6  $\mu\text{m}$  size was placed in the CSTR and pure hydrogen was introduced at a flow rate of 60 NL/h. The reactor temperature was increased from room temperature to 400°C at a rate of 1°C/min, maintained at this activation condition for 24 h and the catalyst was reduced in situ. After the activation period, the reactor temperature was decreased to 120°C. Pure melted  $\text{C}_{28}$  paraffin wax was used as start-up media.  $\text{C}_{28}$  paraffin wax was degassed at degasser vessel with nitrogen at 120°C for 1 h and transferred to the CSTR to be mixed with the catalyst. Then the reactor temperature increased to 180°C under flowing hydrogen. Two separate mass flow controllers (Brooks 5850) were used to add  $\text{H}_2$  and CO at the desired rate to a mixing vessel that was preceded by a lead oxide-alumina containing vessel to remove metal carbonyls before entering to the reactor.

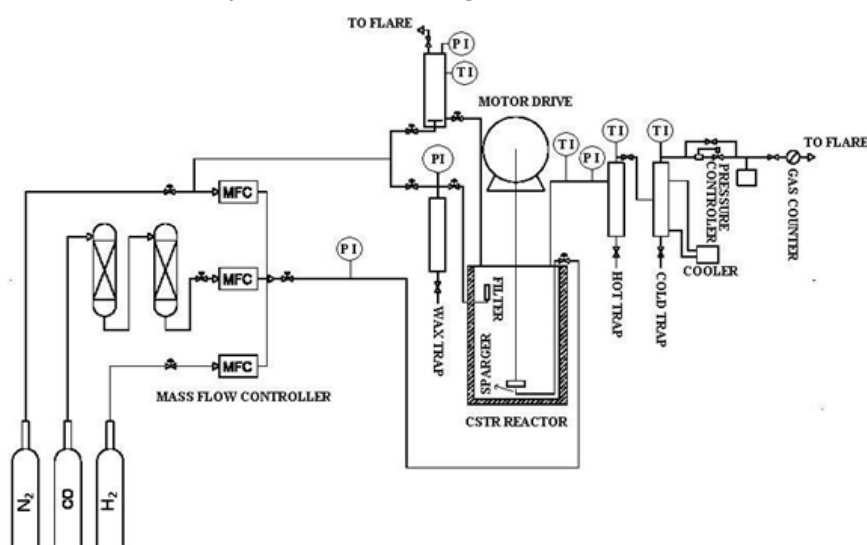


Figure 1. Experimental setup

The mixed gases entered through a dip tube to the bottom of the CSTR below the stirrer. The CSTR was operated at 750 rpm. The temperature of the reactor was controlled via a PID temperature controller. Synthesis gas with a flow rate of 90 NL/h ( $\text{H}_2/\text{CO}$  ratio of 2) was introduced and the reactor pressure was increased to 2.5 MPa. The reactor temperature was then increased to 220°C at a rate of 1°C/min. Products were continuously removed from the vapor and passed through two traps, one maintained at 100°C (hot trap) and the other at 0°C (cold trap). The uncondensed vapor stream was reduced to atmospheric pressure through a pressure letdown valve. The flow was measured with a bubble-meter and composition of outlet gas quantified using a gas chromatograph (Varian CP-3800) equipped with TCD and FID detectors. The  $\text{CO}$ ,  $\text{CO}_2$ ,  $\text{N}_2$ , and  $\text{O}_2$  were analyzed through two packed columns in series (Molecular sieve 13x CP 81025 with 2 m length, and 3 mm OD, and Haysep Q CP1069 with 4 m length, and 3 mm OD) connected to TCD detector. The  $\text{C}_1$ – $\text{C}_5$  hydrocarbons were analyzed via a capillary column (CP fused silica with 25 m $\times$ 0.25 mm $\times$ 0.2  $\mu\text{m}$  film thickness) connected to FID detector. Hydrogen was analyzed through Shimadzu, GC PTF 4C, equipped with TCD detector and two column in series (Propack-Q with 2 m length, and 3 mm OD for  $\text{CO}_2$ ,  $\text{C}_2\text{H}_4$  and  $\text{C}_2\text{H}_6$  separation and molecular sieve-5A with 2m length, and 3mmOD for  $\text{CO}$ ,  $\text{N}_2$ ,  $\text{CH}_4$  and  $\text{O}_2$  separation), which were connected to each other via a three way valve.

The accumulated reactor liquid wax products were removed every 12 h by passing through a 2  $\mu\text{m}$  sintered metal filter located above the liquid level in the CSTR. Also the contents of hot

and cold traps removed every 12 h, the hydrocarbon and water fractions separated, and the collected liquid (Including hydrocarbons and oxygenates) were analyzed offline with Varian CP-3800 gas chromatograph equipped with capillary column (TM DH fused silica capillary column, PETRO COL 100 m×0.25 mm×0.5 μm film thickness) connected to FID detector. Both total mass and atomic material balances were performed with the consideration that a run could be accepted for further analysis if the carbon material balance closed between 97 and 103%. This criterion was adopted, since compounds containing carbon and hydrogen may accumulate in the reactor in the form of high molecular weight hydrocarbons.

The CO conversion, FTS rate (g HC/g cat./h), and selectivity of hydrocarbon products are defined due to formula presented in our previous work [11-12].

### 3. Result and discussion

#### 3.1. Alumina-support characterization

Results of the BET surface area measurements are shown in Figures 2 A and B. These characterizations clearly show the changes of morphology (surface area, pore volume, pore size distribution and crystallite phase) of the supports. Heat and mass transfer of reactants and products were facilitated by phosphor-doped alumina-supported cobalt catalysts, via creating larger pores, increase hydrothermal stability and decrease deactivation rate of catalysts in FTS reaction.

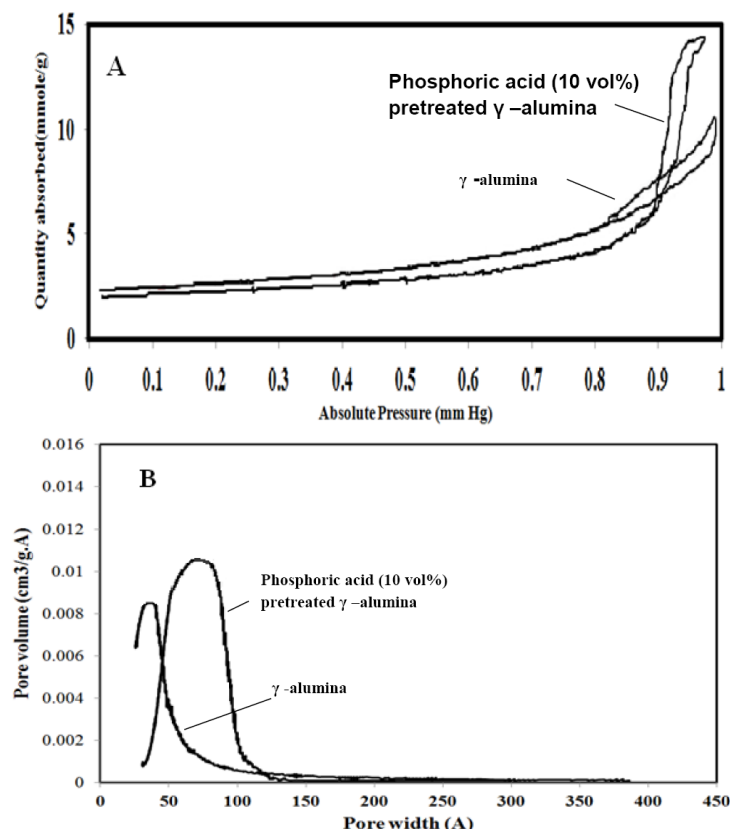


Figure 2. A) Adsorption-Desorption isotherm of supports B) Pore size distribution of supports

#### 3.2. Catalyst characterization

The elemental compositions of all calcined catalysts were shown in Table 1. The ICP-MS results indicated that most of elements were deposited on the supports during incipient wetness impregnation.



The FTIR absorption spectrums of all catalysts (ALCR, ALC<sub>1</sub>-ALC<sub>3</sub>) are shown in Figure 3. The extended band around 3500 cm<sup>-1</sup> and the band around 1630 cm<sup>-1</sup> can be attributed to the O-H stretching frequency and the presence of H<sub>2</sub>O vibration respectively. The presence of band in 1118 cm<sup>-1</sup> can be attributed to O-P-O stretching-vibration band and with increasing the amount of phosphor-doped in support the intensity of this band is increased due to more formation of aluminum phosphate. The presence of band in 665 cm<sup>-1</sup> and 569 cm<sup>-1</sup> can be attributed to Co-O band [13].

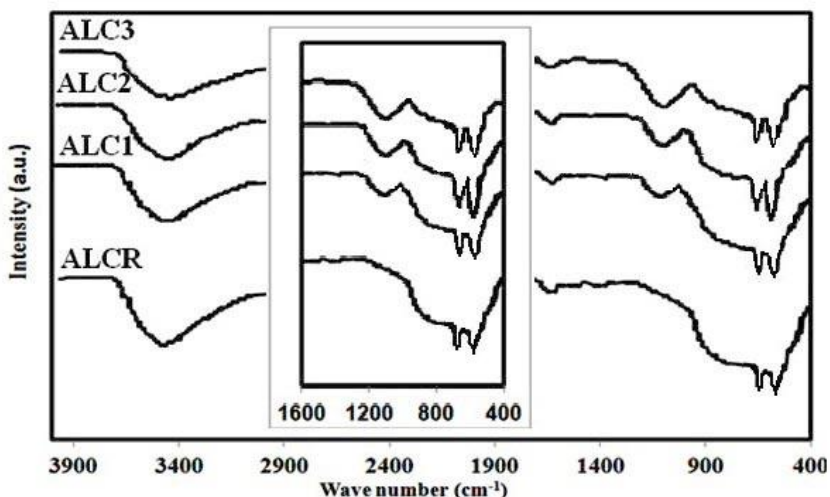


Figure 3. FTIR spectrum of calcined catalysts

The size of the particles and morphology of the surface of the support were also determined using TEM images. The TEM images of the catalysts made by impregnation are shown in Figure 4.

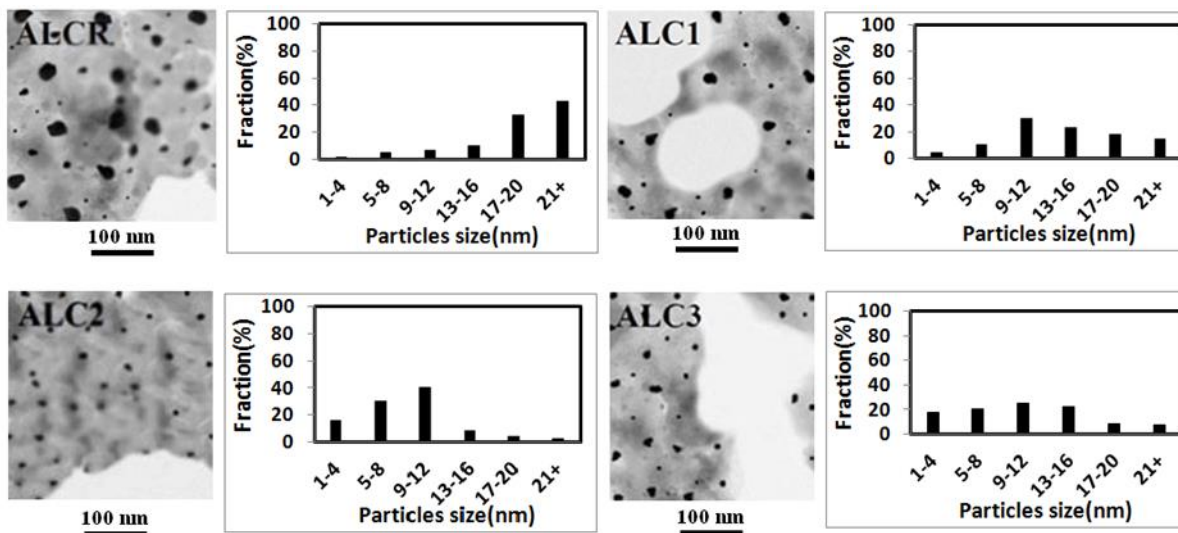


Figure 4. TEM images of the calcined catalysts

TEM images of these catalysts show some black spots correspond to the cobalt particles. Figure 4 also depicts the size distribution of the metal particles (approximately 100 particles), which is determined using the population of the total metal particles of each catalyst based on data taken from different TEM images (four images were presented here). According to TEM images of catalysts, modified  $\gamma$ -alumina produced small particles which are uniformly dispersed on the support [14]. This figure shows that metal nanoparticle size distributions for the catalysts prepared with modified  $\gamma$ -alumina (ALC<sub>1</sub>-ALC<sub>3</sub>) are better compared to the catalyst prepared

on conventional  $\gamma$ -alumina (ALCR). TEM images demonstrate the uniformity of the crystallites in ALC<sub>2</sub> catalyst and the metal particles size within a narrow range can be observed through this catalyst. According to Figure 4, the average particle sizes for ALCR and ALC<sub>1</sub>-ALC<sub>3</sub> catalysts are about 18.10, 15.64, 10.16 and 14.22 nm, respectively.

Results of the surface area measurements are shown in Table 1. These results show that the BET surface area of ALCR catalyst decrease due to some alumina pore blockage by cobalt active phase impregnated on it. In case of ALC<sub>2</sub>, this event was occurred lower, because of uniform distribution of cobalt particles leading to optimization of cobalt particle sizes which pores filling have occurred mostly in this case. In ALC<sub>3</sub> and ALC<sub>2</sub> catalysts the uniformity of cobalt particles are lower than ALC<sub>1</sub> and so both of pore filling and blockage have occurred.

XRD diffractograms of the calcined catalysts are shown in Figure 5. In the XRD patterns the peaks at  $2\theta$  values of  $25^\circ$  and  $43^\circ$  correspond to the  $\gamma$ -alumina support, while other peaks in the spectra of the catalysts are related to different crystal planes of Co<sub>3</sub>O<sub>4</sub> [15]. The peak at  $2\theta$  value of  $36.8^\circ$  is the most intense one of Co<sub>3</sub>O<sub>4</sub> in XRD spectrum of all catalysts. Minor peaks were also observed at  $44^\circ$ , and  $52^\circ$  for the catalysts which correlate with a cubic cobalt structure [5]. Table 1 reports the average Co<sub>3</sub>O<sub>4</sub> particle size of the catalysts calculated from XRD diffractograms using the Scherer equation at  $2\theta$  value of  $36.8^\circ$  [16]. The average Co<sub>3</sub>O<sub>4</sub> cluster size was determined after calcinations for the ALC<sub>1</sub>-ALC<sub>3</sub>, ALCR as approximately 16.6, 11.5, 14.4 and 18.8 nm, corresponding to 12.45, 8.6, 10.8 and 13.8 nm when reduced to metal, respectively. These agree reasonably well with the cobalt particle diameters obtained with the H<sub>2</sub> chemisorption results (Table 2).

Table 2. H<sub>2</sub>-TPD results

Sample	$\mu$ mole H <sub>2</sub> desorbed /g cat.	$\mu$ mole O <sub>2</sub> consumed /g cat.	Reduction degree(%) <sup>a</sup>	Dispersion (%) <sup>b</sup>	H <sub>2</sub> -TPD $d_{Co^0}$
ALC <sub>1</sub>	287	1242	56	11.1	10.6
ALC <sub>2</sub>	386	2085	69	14.6	7.3
ALC <sub>3</sub>	327	1469	62	12.1	9.8
ALCR	253	1007	50	9.6	11.4

<sup>a</sup> Determined by TPR from  $0^\circ\text{C}$  to  $800^\circ\text{C}$  according to ref. [5] ; <sup>b</sup> Determined according to ref. [5]

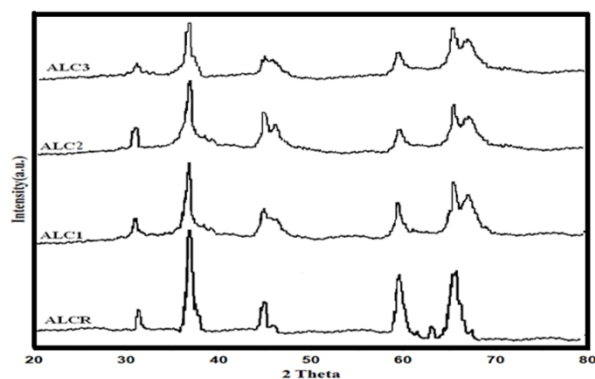


Figure 5. XRD diffractograms of calcined catalysts

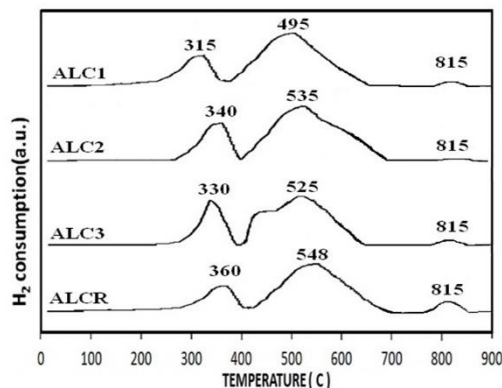


Figure 6. TPR patterns of the calcined catalysts from 30 to  $850^\circ\text{C}$

The reducibility of the catalysts in H<sub>2</sub> atmosphere was determined by TPR experiments. The TPR spectra of the calcined ALC<sub>1</sub>-ALC<sub>3</sub>, ALCR are shown in Figure 6. The low temperature peak ( $300\text{--}380^\circ\text{C}$ ) is typically assigned to reduction of Co<sub>3</sub>O<sub>4</sub> to CoO, although a fraction of the peak likely comprises the reduction of the larger, bulk-like CoO species to Co<sup>0</sup> [12,15-16]. The second broad peak is assigned to reduction of small CoO to Co<sup>0</sup> species, which also includes the reduction of cobalt species that interact with the support.

According to Figure 6, the deposition of cobalt nanoparticles synthesized on the modified  $\gamma$ -alumina for ALC<sub>1</sub>-ALC<sub>3</sub> catalysts shift the reduction peaks to a lower temperature compared to the catalyst prepared by conventional  $\gamma$ -alumina. Interestingly, the reduction temperature peaks decreases sensibly with decreasing cobalt particle size from 16.6 to 11.5 nm (ALC<sub>1</sub>-ALC<sub>2</sub>). This phenomenon can be attributed to higher reducibility for cobalt particles produced in this special method through formation of the functional group on  $\gamma$ -alumina surface as a site of interaction. This functional groups have obstructed the sintering of cobalt, promoted activating hydrogen or accelerated the hydrogen spill-over effect under the reduction process, contributing to realizing higher dispersion and reduction degree of these catalysts simultaneously [12,16-17]. But in case of ALC<sub>1</sub>-ALC<sub>3</sub>, the high dispersion of cobalt particles and decreasing the size of them increased the reduction degree of catalyst, the interactions between support and active phase, and the reduction temperature peaks. Thus, particles within the modified  $\gamma$ -alumina are easily reduced because of the functional group effect, but the reducibility is still more influenced by the particle size.

As shown in Figure 6, there is formation of metal-support compounds on the catalyst surface due to reduction peaks above 500°C. Tavasoli *et al.* [2] have noted that reduction peak present at temperatures above 700°C with oxidic carrier shows formation of cobalt species that are difficult to reduce (oxide compounds). The formation of cobalt aluminate in ALC<sub>1</sub>-ALC<sub>3</sub> catalysts decreases compared to ALCR because of interactions of cobalt active phase with aluminum phosphate [13,18].

The results of the temperature programmed desorption (TPD) of the hydrogen for ALC<sub>1</sub>-ALC<sub>3</sub> and ALCR catalysts were reported in Table 2. This table shows that in case of ALC<sub>1</sub>-ALC<sub>3</sub> catalysts, the hydrogen chemisorption (H<sub>2</sub> uptake) increases with decreasing the cobalt particle sizes up to 7.3 nm in accordance with the % dispersion of the cobalt particles. Thus, decreasing the cobalt particle size increases the % dispersion from 9.6 to 14.6 % (see Table 2).

The H<sub>2</sub> uptakes of the ALC<sub>1</sub>-ALC<sub>3</sub> catalysts are higher than the ALCR catalyst. It has been shown that narrow particle size distributions are efficient for H<sub>2</sub> chemisorption [6]. Also it can be related to formation of the functional group on modified  $\gamma$ -alumina surface, which promoted activating hydrogen or accelerated the hydrogen spill-over effect under the reduction process, contributing to realizing higher dispersion and reduction degree of these catalysts simultaneously [10,16].

### **The effects of acetic acid pretreatment**

To investigate the promotional role of phosphoric acid in pretreatment support, the catalytic activity and product selectivity data have been calculated for runs showing catalyst stability within the first 320 h of FTS operation and were repeated twice to confirm the results reproducibility. After initial catalyst stability, the results of FTS rate (g HC produced/g cat./h), and the percentage CO conversion at 220°C, 2.5 MPa, and H<sub>2</sub>/CO ratio of 2 for ALC<sub>1</sub>-ALC<sub>3</sub> catalysts and ALCR catalysts have been calculated.

The comparative results of CO conversion, FTS rate (g HC produced/gcat./h), C<sub>5</sub><sup>+</sup> and CH<sub>4</sub> selectivity for ALC<sub>1</sub>-ALC<sub>3</sub> and ALCR catalysts are presented in Figures 7 (A, B, C and D). In case of ALC<sub>1</sub>-ALC<sub>3</sub> catalysts, the higher distributed of cobalt particles were caused the CO conversion became higher than the ALCR catalyst. The ALC<sub>2</sub> catalyst showed higher and stable CO conversion (during 120-320 h of TOS). This can be attributed to higher uniformity of particle size distribution and inhibiting the formation of cobalt aluminate through interaction of cobalt and surface support (aluminum phosphate) in FTS reaction and in presence of water as a side reaction product. On the other hand, phosphor-doped alumina inhibits cobalt oxidation, facilitates heat and mass transfer by using larger pores (as shown in Figures 2 A and B), which increase hydrothermal stability and decrease deactivation rate of catalysts in FTS reaction [13-14,17-18].

According to Figure 7 (B, C, D), the proposed modified  $\gamma$ -alumina supported catalysts increased the FTS rate from 0.062 to 0.1195 g HC/gcat./h, C<sub>5</sub><sup>+</sup> selectivity increased 10% and CH<sub>4</sub> selectivity decreased 73%, compared to that prepared by conventional  $\gamma$ -alumina support. ALC<sub>2</sub> catalyst showing narrow and uniform particle size distribution compared to ALCR catalyst.



Because of uniformity, the cobalt sites produced on ALC<sub>2</sub> catalyst are more catalytically active than the ones produced on ALCR [13-14,17-18]. These phosphorus doped alumina act as anchoring sites for metal particles on surface of alumina. Also they can affect metal dispersion and stability of active metallic sites [20] through interaction of active phase with alumina phosphate and inhibiting the formation of cobalt aluminate [14,18].

Chen *et al.* observed that particle size is not the only property to have an effect on the FTS activity [19]. Other researcher observed that a narrow particle size distribution enhances the activity of the FTS catalysts, which in turn leads to a better conversion of the reactants as well as an increase in the FTS rate [20]. Thus, improvement of the uniformity of the cobalt particles supported on phosphorus doped alumina leads to a better CO conversion, stability of the products, and the FTS activity and selectivity.

The C<sub>5</sub><sup>+</sup> selectivity and CH<sub>4</sub> selectivity have increased and decreased respectively in modified  $\gamma$ -alumina-supported cobalt catalysts (ALC<sub>1</sub>-ALC<sub>3</sub>) compared to ALCR catalyst. ALC<sub>2</sub> catalyst showed lower selectivity to methane. Lower production rate of CH<sub>4</sub> for this catalyst could be due to the effective participation of olefins in the carbon-carbon chain propagation. Thus, on the ALC<sub>2</sub> catalyst, the larger pore volume and the better pores structure and shape (as shown in Figures 2 A and B) facilitate heat and mass transfer and cause the  $\alpha$ -olefins of the type R-CH=CH<sub>2</sub> can compete with carbon monoxide and heavier olefins for re-adsorption and chain initiation [20-22]. The selectivity for C<sub>5</sub><sup>+</sup> products on the modified  $\gamma$ -alumina supported cobalt catalysts (ALC<sub>1</sub>-ALC<sub>3</sub>), are higher than conventional  $\gamma$ -alumina supported-cobalt catalyst (ALCR) considering the same reason mentioned above. The uniformity and more distributed of cobalt particles in ALC<sub>2</sub> catalyst caused the C<sub>5</sub><sup>+</sup> selectivity became higher than ALC<sub>1</sub> and ALC<sub>3</sub>. The particle sintering is effectively prevented inside modified  $\gamma$ -alumina due to spatial restriction of the  $\gamma$ -alumina pores which stabilized the activity and selectivity of the cobalt particles [22-24].

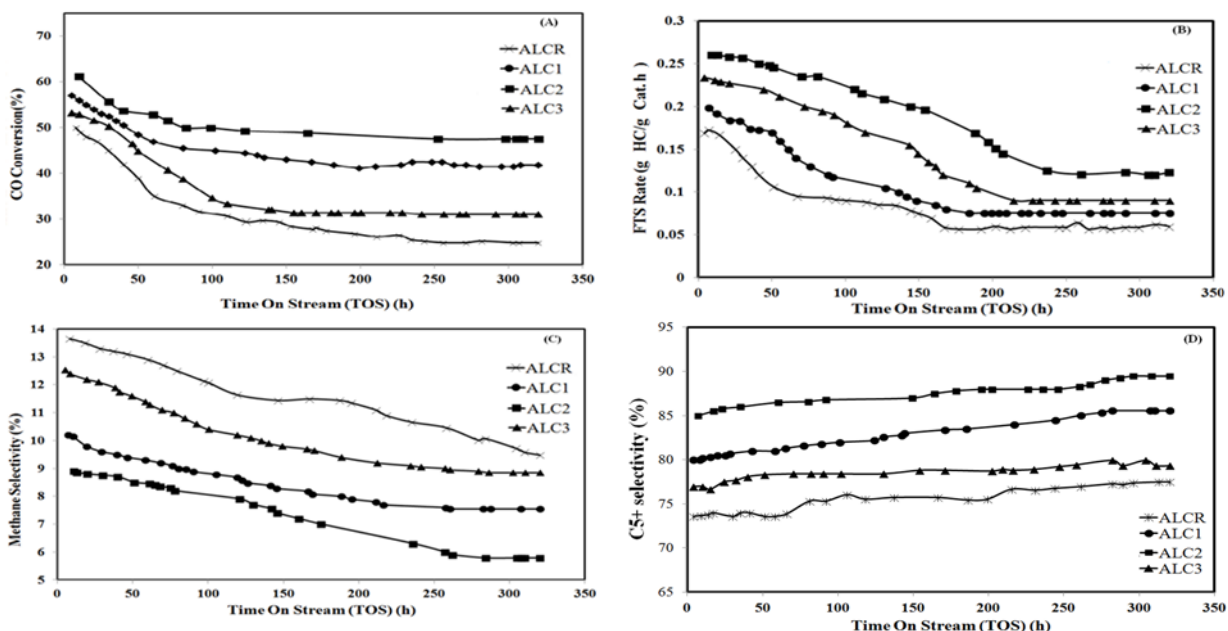


Figure 7. A) CO conversion B) FTS rate C) CH<sub>4</sub> selectivity D) C<sub>5</sub><sup>+</sup> selectivity of the calcined catalysts (Wt. of catalyst=10 g, T=220°C, P=2.5 MPa, and H<sub>2</sub>/CO ratio of 2)

#### 4. Conclusions

The promotional effects of solvent during the preparation of FTS catalyst were investigated. The phosphoric acid modified the morphology of support (surface area, pore volume, pore size distribution and crystallite phase) and formed new functional group on  $\gamma$ -alumina surface. The modified surface properties of  $\gamma$ -alumina support realized high dispersion and reduction

degree of supported cobalt simultaneously, contributing to higher catalytic activity and stability of this kind of catalyst applied to FTS reaction in CSTR reactor during 320 h test. Synthesis of highly dispersed and stable cobalt catalysts caused high activity and stability of this catalyst through interaction of active phase with alumina phosphate and inhibiting the formation of cobalt aluminate. It is found that dilemma of dispersion and reducibility of  $\gamma$ -alumina-supported cobalt catalyst would be easily resolved via reconstructing the surface properties of supports by various solvent, such as phosphoric acid, during preparation of catalyst. Pretreated  $\gamma$ -alumina as a catalyst support of cobalt nanoparticles, maintain high dispersion and reducibility of cobalt, which can be attributed to hydrogen spill-over effect of functional groups on modified  $\gamma$ -alumina surface. This event will not normally occur in catalyst prepared by conventional  $\gamma$ -alumina. The simultaneously improved dispersion and reducibility of  $\gamma$ -alumina-supported cobalt nanoparticles would contribute to forming more active site on catalysts, which is advantageous to any structure-insensitive reaction.

## Acknowledgements

The author is thankful to the Iran National Science Foundation for their funding support of this work.

## References

- [1] Bezemer GL, Bitter JH, Kuipers HPCE, Oosterbeek H, Holewijn JE, Xu X, Kapteijn F, van Dillen AJ, de Jong KP. J. Am. Chem. Soc. 128 (2006) 3956-3964.
- [2] Tavasoli A, Abbaslou RM M, Trepanier M, Dalai AK. Appl. Catal. A 345 (2008) 134-142.
- [3] Li J, Jacobs G, Zhang Y, Das T, Davis BH. Appl. Catal. A: General 223 (2002) 195-203.
- [4] Dry ME. J. Chem. Tech. Biotech. 77 (2001) 43-50.
- [5] Jacobs G, Das TK, Zhang Y, Li J, Racollet G, Davis BH. Appl. Catal. A 233 (2002) 263-281.
- [6] Iglesia E, Soled SL, Fiato RA. J. Catal. 137 (1992) 212-224.
- [7] Johnson BG, Bartholomew CH, Goodman DW. J. Catal. 128 (1991) 231-247.
- [8] Tavasoli A, Mortazavi Y, Khodadadi AA, Sadagiani K, Karimi A. I. J. Chem. Chem. Eng. 35 (2005) 9-15.
- [9] van Berge PJ, van de Loosdrecht J, Barradas S, van der Kraan AM. Catal. Today 58 (2000) 321-334.
- [10] Zhang J, Chen J, Ren J, Sun Y. Applied Catalysis A: General 243 (2003) 121-133.
- [11] Karimi A, Pour AN, Torabi F, Hatami B, Alaei M, Irani M. J. Nat. Gas Chem. 19 (2010) 503-508.
- [12] Karimi A, Nassernejad B., Rashidi AM. Fuel 117( 2014) 1045-1051.
- [13] Tiitta M, Nykanen E, Soininen P, Niinisto L, Leskela M, Lappalainen R. Mat. Res. Bull. 33 (1998) 1315-1323.
- [14] da Costa P, Potvin C, Manoli JM, Breyse M, Djega-Mariadassou G. Catal. Lett. 72 (2001) 91-97.
- [15] Trépanier M, Tavasoli A, Dalai AK, Abatzoglou N. Appl. Catal. A 353 (2009) 193-202.
- [16] Abbaslou RMM, Tavasoli A, Dalai AK. Appl. Catal. A: General 355 (2009) 33- 41.
- [17] Jacobs G, Das TK, Zhang Y, Li J, Racollet G, Davis BH. Appl. Catal. A: General 233 (2002) 263-281.
- [18] Jong-Wook Bae, Seung-Moon Kim, Yun-Jo Lee, Ki-Won Jun, US patent 8598066 B2 (2013).
- [19] Chen W, Fan Z, Pan X, Bao X. J. Am. Chem. Soc. 130 (2008) 9414-9419.
- [20] Trépanier M, Dalai AK, Abatzoglou N. Appl. Catal. A: General 374 (2010) 79-86.
- [21] van Steen E, Sewell GS, Makhothe RA, Micklethwaite C, Manstein H, de Lange M, O'Connor CT. J. Catal. 162 (1996) 220-229.
- [22] Pan X, Fan Z, Chen W, Ding Y, Luo H, Bao X. Nature 6 (2007) 507-511.

- [23] Terörde RJAM. Ph.D. Thesis-Utrecht University-Utrecht, Netherlands (1996).
- [24] Davari M, Karimi S, Tavasoli A, Karimi A. Enhancement of activity, selectivity and stability of CNTs-supported cobalt catalyst in Fischer-Tropsch via CNTs functionalization. Appl. Catal A: General, under press.

---

*\*Corresponding author; Email: karimial@ripi.ir; Tel.: +982148252395; Fax: +982144739716*